

MICROWAVE BACKGROUND: PHENOMENOLOGY AND OBSERVATIONS

G. JUNGMAN

ABSTRACT. This third lecture on the μ -wave background radiation discusses the phenomenology of temperature fluctuation measurements and the current state of the observations.

CONTENTS

1. Sky Multipoles	1
1.1. Review of Temperature Multipoles	1
1.2. Correlation Function and Power	2
1.3. Microwave Background as a Linear Filter	2
1.4. Cosmic Variance	3
2. Simplified Picture of Observations	4
3. Cosmic Parameters	5
3.1. Ω	5
3.2. Other Stuff	7
4. COBE	7
5. BOOMERANG	8
6. MAP	8
7. PLANCK	9
8. Polarization	9
References	11

1. SKY MULTIPOLES

1.1. Review of Temperature Multipoles. First we briefly recall the spherical harmonic expansion of temperature variation on the sky. Specializing to a frame co-moving with the Earth, we wrote an expansion for the observed

temperature variation in the form

$$\frac{\Delta T}{T}(\theta, \phi) = \delta_T(\theta, \phi) = \sum_{l=1}^{\infty} \sum_{m=-l}^l a_{lm} Y_{lm}(\theta, \phi).$$

The signal on the full sky can always be represented in this form.

1.2. Correlation Function and Power. The two-point correlation function on the sky is a function of angular separation defined by

$$\begin{aligned} C(\theta) &= \langle \delta_T(e_1) \delta_T(e_2) \rangle_{e_1, e_2, e_1 \cdot e_2 = \cos \theta} \\ &= \sum_{l, m} \sum_{l', m'} a_{lm}^* a_{l'm'} \langle Y_{lm}^*(e_1) Y_{l'm'}(e_2) \rangle_{e_1, e_2, e_1 \cdot e_2 = \cos \theta} \end{aligned}$$

If we define coefficients c_l as in the second lecture,

$$c_l = \frac{1}{2l+1} \sum_{m=-l}^l |a_{lm}|^2,$$

then the correlation function can be written

$$C(\theta) = \frac{1}{4\pi} \sum_{l=1}^{\infty} (2l+1) c_l P_l(\cos \theta).$$

The correlation function at coincident points is interesting since it encodes the average point-wise fluctuation on the sky.

$$\begin{aligned} C(0) &= \langle \delta_T(e) \delta_T(e) \rangle_e \\ &= \sum_l (2l+1) c_l. \end{aligned}$$

Each c_l is a sum of squares of amplitude coefficients, and the power associated with a given multipole is $l(l+1)c_l$. Therefore we can think of the c_l as defining a power spectrum of excitations as a function of multipole moment. This is the fundamental observable for the temperature fluctuation signal.

1.3. Microwave Background as a Linear Filter. As we saw, the complete dynamical system which describes the growth of radiation temperature fluctuations is linear. Therefore the signal on the sky is some linear function of the initial amplitude function, so without loss we can write

$$\delta_T(\vec{e}) = \int d\mu(\vec{k}) \mathcal{A}(\vec{k}) g(\vec{k} \cdot \vec{e}),$$

for some function g , where we assumed that the underlying dynamical process is rotationally invariant. Then we can express the amplitude coefficients a_{lm} as

$$a_{lm} = \int d\mu(\vec{k}) T_{lm}(k) \mathcal{A}(\vec{k}),$$

where we introduced a kind of generalized transfer function,

$$T_{lm}(k) = \int d\Omega(\vec{e}) g(\vec{k} \cdot \vec{e}) Y_{lm}(\vec{e}).$$

1.4. Cosmic Variance. When discussing inflation we introduced the idea of stochastic initial conditions; the Universe represents one realization of an ensemble of possible universes. If this ensemble is assumed Gaussian and isotropic, then it is completely characterized by a rotationally invariant two-point function. We further assume the correlation function is local; therefore we can write

$$\langle \mathcal{A}^*(\vec{k}_1) \mathcal{A}(\vec{k}_2) \rangle = A(k_1) \delta(\vec{k}_1 - \vec{k}_2).$$

Then the ensemble average of the harmonic coefficient functions is given by

$$\begin{aligned} \langle a_{lm}^* a_{l'm'} \rangle &= \int d\mu(k) T_{lm}^*(k) T_{l'm'}(k) A(k) \\ &= \int d\Omega(e) \int d\Omega(e') Y_{lm}^*(e) Y_{l'm'}(e') \int d\mu(k) A(k) g(\vec{k} \cdot \vec{e}) g(\vec{k} \cdot \vec{e}') \\ &= \int d\Omega(e) \int d\Omega(e') Y_{lm}^*(e) Y_{l'm'}(e') G(e \cdot e'). \end{aligned}$$

$G(e \cdot e')$ is defined as the result of the momentum integration appearing in the second line. Expand G in Legendre polynomials,

$$G(e \cdot e') = \sum_l b_l P_l(e \cdot e'),$$

and use the addition theorem,

$$P_l(e \cdot e') = \frac{4\pi}{2l+1} \sum_{m=-l}^l Y_{lm}^*(e') Y_{lm}(e).$$

Therefore

$$\begin{aligned} \langle a_{lm}^* a_{l'm'} \rangle &= \int d\Omega(e) \int d\Omega(e') Y_{lm}^*(e) Y_{l'm'}(e') \sum_{\lambda\mu} b_\lambda \frac{4\pi}{2\lambda+1} Y_{\lambda\mu}^*(e') Y_{\lambda\mu}(e) \\ &= \frac{4\pi}{2l+1} b_l \delta_{ll'} \delta_{mm'}. \end{aligned}$$

So we get the relatively simple result that the a_{lm} are independent random variables. If the spectrum of input fluctuations is Gaussian, then the a_{lm} are Gaussian, and thus completely characterized by the second moment calculated here. In this case the c_l are sums of squares of Gaussian random variables. Given the Gaussian nature of the a_{lm} , it is easy to calculate the probability distribution of c_l values. A little algebra gives

$$f(c_l)dc_l = \frac{(l + \frac{1}{2})^{l+\frac{1}{2}}}{(\bar{c}_l)^{l+\frac{1}{2}}} \frac{1}{\Gamma(l + \frac{1}{2})} c_l^{l-\frac{1}{2}} \exp\left(-\frac{(l + \frac{1}{2})c_l}{\bar{c}_l}\right)$$

Here \bar{c}_l is the mean of the distribution. As this shows, the dispersion is related to the mean, and the distribution becomes sharper with increasing l . Within the stochastic theory of initial conditions, this sample variance is an absolute limitation to the power of observations. It is called *cosmic variance*.

2. SIMPLIFIED PICTURE OF OBSERVATIONS

Any real experiment has at least three complicating features. First, real antenna patterns lead to finite resolution, with a resolution function that depends on details of the experiment design. Again, everything is linear, so we can account for this effect by introducing an l dependent *window function*, W_l . The expression for the correlation function becomes

$$C(\theta) = \frac{1}{4\pi} \sum_{l=1}^{\infty} (2l + 1) c_l P_l(\cos \theta) W_l.$$

Because window functions represent the effect of finite angular resolution, they all fall off at large l . For example, the COBE window function was modeled as

$$W_l^{COBE} = \exp\left[-\left(l + \frac{1}{2}\right)^2 \sigma^2\right], \quad \sigma \simeq 0.074.$$

This gives a half-maximum cutoff around $l \simeq 12$ or roughly 10 degrees. The form corresponds to a Gaussian beam profile.

The second issue is noise. A sky map is made by pixelizing the sky and integrating the signal in different pixels over time. Each pixel in a map has some characteristic noise component. Because the observational strategy will generally lead to inhomogeneous coverage on the sky, pixels have different histories and different noise characteristics. Note that this pixel noise is purely local on the sky, whereas the signal is always interpreted as a function of l . However, for formal purposes we can expand the noise signal in

the same way and model the observed signal as

$$C_{OBS}(\theta) = \frac{1}{4\pi} \sum_l (2l + 1) [c_l W_l + c_l^{NOISE}] P_l(\cos \theta).$$

Notice that the noise does not carry a factor of the window function since it has nothing to do with the sky. Therefore, when the window function drops off, the observed signal becomes noise dominated.

The third issue is foreground sources. For example, dust emission in the plane of the Galaxy must be modeled and subtracted in the analysis. Such foregrounds are an important systematic. Synchrotron and free-free emissions can be dealt with similarly. Ground-based experiments must also deal with various antenna systematics due to ground emission.

Given this type of modeling, one typically attempts a maximum-likelihood analysis to extract the signal parameters, the cosmological c_l . When the c_l are given by calculations in a cosmological model, the results are interpreted as giving cosmological parameters in a maximum-likelihood sense.

One final issue is sky coverage. A ground-based or balloon-borne experiment typically sees only a fraction of the full 4π sky. Space-based experiments must work with cut portions of the sky because of foreground removal. This is an important point for data analysis, because all the formulae derived above depend on full-sky coverage; it is assumed that the signal can be analyzed into spherical harmonics, which require full sky coverage. With incomplete sky coverage, it is not possible to fully distinguish the spherical harmonic components. This means that the $\{c_l\}$ values determined by such an experiment are not statistically independent since they do not represent orthogonal components of the signal. In such a situation we cannot speak about the error in a single c_l value, but we must speak about the covariance of the full set of values. Typically this covariance dies off for l separated by some Δl ; this "correlation length" for l values is sometimes called the l "resolution" for the experiment.

3. COSMIC PARAMETERS

3.1. Ω . There is a very pretty way to use the microwave background to determine the spatial curvature of the Universe. It relies on the fact that the physical scale of acoustic waves at the time of decoupling is a fixed parameter; in particular, the acoustic horizon is determined solely by the speed of sound in the medium and the elapsed time (the age of the Universe) at recombination. The first Doppler peak in the c_l power spectrum comes from the fundamental mode which lives right inside this acoustic horizon. Therefore the position of the first peak in l space should be related directly to the

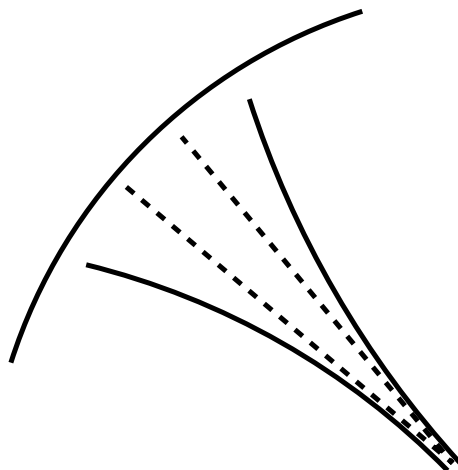


FIGURE 1. Relation between apparent angular size and transverse distance in an open universe. The solid curves are the paths that light travels to get to the observation point. The dotted lines are the paths that would be followed in a universe with flat spatial sections, which lead to smaller inferred transverse length scales on the fixed surface.

size of the acoustic horizon. This gives a location of $l_1 \simeq 200$. Remember that the width of this peak is not small, although it appears localized when plotted versus $\log l$. But the peak is a well-defined point, and the shape is understood theoretically.

But if the Universe is curved, we have to be more careful about the trigonometry. Suppose the Universe is open, with spatial sections of negative curvature. Then parallel lines, and therefore the spacelike projections of null geodesics, diverge from each other as they leave a point. The rays entering your eye also diverge as we follow them backward onto the sky. Therefore, the apparent angular separation of points on the sky is less than the "actual" angle subtended on some surface of fixed time in the past. This effect is expressed by the formula for angular diameter distance which we have seen previously.

So in an open Universe we calculate that the Doppler peaks must move to higher l . In particular, the position of the first peak is a robust measure of the apparent size of the acoustic horizon, and therefore of the curvature of the Universe.

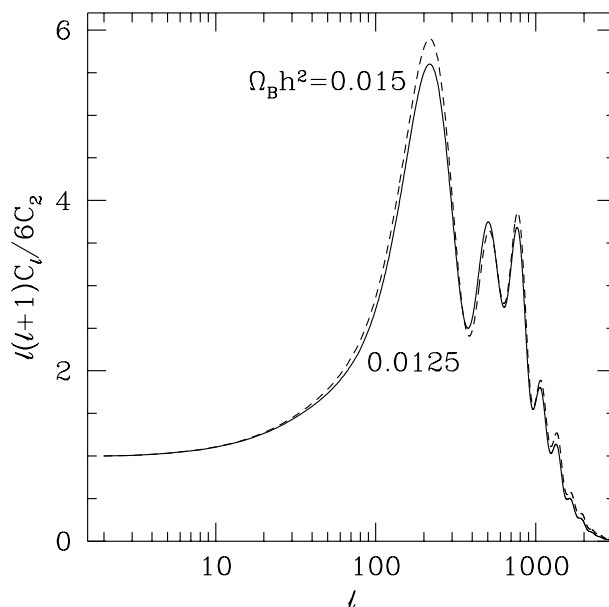


FIGURE 2. Variation in power spectrum due to changes in the baryon fraction. Taken from Ref. [HSSW95]

3.2. Other Stuff. All aspects of the multipole power spectrum are controlled by basic physics which we understand. This physics is itself controlled by the physical inputs, such as fundamental cosmological parameters. For example, these include the baryon ratio Ω_B and the Hubble constant h . As part of a full likelihood analysis one can determine values for these parameters.

For example, consider the baryon density. Obviously changes in the baryon density cause changes in the equation of state of the photon-baryon fluid. In particular, higher baryon densities mean less pressure, so that gravitational collapse can create stronger compression of the fluid. Similarly, the rarefactions are driven to smaller amplitude. The first acoustic peak represents power in fundamental compression waves, but the second peak corresponds to power in rarefaction waves. This pattern repeats for odd and even peaks. Therefore the best way to get information about $\Omega_b h^2$ is to examine the relative heights of the different acoustic peaks.

4. COBE

COBE provided our first confirmed detection of the temperature anisotropy for $l \geq 2$. The satellite carried several instruments, including a differential microwave radiometer (DMR). The DIRBE instrument measured infrared

emission; its maps of dust emission were used to create cuts for infrared foregrounds. The DMR operated at frequencies of 31.5 GHz, 53 GHz, and 90 GHz.

The COBE angular resolution was approximately 8 degrees; a model window function was introduced above. This means that COBE was completely unable to detect the structure at higher l .

In a certain sense COBE fixes the overall normalization of the power spectrum. Note that there are two different ways to characterize this normalization. The directly measured COBE quadrupole is $Q = 10.7 \pm 3.6 \pm 7.1 \mu K$. But it is better to use an average taking into account the values of all the measured multipoles, which gives $Q_{PS} = 15.3^{+3.8}_{-2.8} \mu K$. The directly measured quadrupole is perhaps a little low compared to the determination from all measured multipoles; this may well be cosmic variance in action.

5. BOOMERANG

BOOMERANG is a balloon-borne experiment which has flown around the Antarctic, targeting an area of low galactic emission in the Southern hemisphere called the Southern Hole. The flight plan uses a prevailing circular wind pattern to circumnavigate the pole. This allows relatively long exposure times, 10 days or longer, more than is possible for a typical balloon experiment.

The instrumentation and strategy allow for temperature sensitivity of $\simeq 20 \mu K$ per pixel and an angular resolution of about $15'$. Some regions are scanned more often, giving a temperature sensitivity of about $\simeq 10 \mu K$ in those regions.

The BOOMERANG data set is quite large, and the analysis required a dedicated supercomputing effort. One analysis [M⁺02] has computed the power spectrum from 150 GHz sky maps, covering about 3% of the sky. The first peak position was found to be $l_1 \simeq 213^{+10}_{-13}$. At 95% confidence the analysis gives $0.85 < \Omega < 1.1$ and $0.36 < \Omega_\Lambda < 0.72$. The analysis also gives an estimate for the baryon density $0.015 < \Omega_b h^2 < 0.029$, which is consistent with big bang nucleosynthesis. Of course, there are correlations in these determinations.

6. MAP

The MAP satellite arrived at the L2 Lagrange point in October of 2001, and is currently taking data. Earlier in April this year (2002) it finished its first full-sky data taking; map making is underway.

The basic parameters for the experiment are the angular resolution, $\Delta\theta \simeq 0.3$ degrees, which corresponds to a maximum l of about 600, and the temperature resolution of about $\Delta T \simeq 20\mu K$ per 0.3 degree-square pixel, with a systematic limit of about $5\mu K$ per pixel. The MAP strategy is to observe at five frequencies and use differencing of the signals at these frequencies to subtract away combinations which have the spectral signature of foreground emissions.

7. PLANCK

PLANCK is the ESA satellite mission for microwave background observation. The PLANCK experiment consists of two separate detector systems, together operating at eight frequencies. The parameters for the instrument illustrate its ambitions. The angular resolution is $\Delta\theta \simeq 7'$, which corresponds to a maximum l of about 1500. The temperature sensitivity should be about $\Delta T/T \simeq 10\mu K$ across the whole sky, with a lower limit of a few μK in selected low background regions.

At the level of sensitivity which is the PLANCK goal, foregrounds will be a very important part of the analysis. The foregrounds will be separated using information from the wide range of observational frequencies.

8. POLARIZATION

Thus far in these lectures nothing has been said about polarization, and very little about gravity waves. It turns out that, from a phenomenological viewpoint, these topics go well together.

The microwave background signal is certainly polarized, due to the angular dependence of Thomson scattering. So far we have ignored this and assumed that the radiation transport happens in an equal mixture of polarization states. It turns out that including polarization has a relatively small effect on the observed temperature signal. However, it does introduce more observables into the picture; we can hope to measure the polarization of the signal and thus obtain more information.

One thing which we learn about from polarization is late-time reionization of the Universe. After the formation of stars, pockets of the Universe become reionized due to UV emissions. The ionization density n_e rises again, above the primordial frozen value which we calculated in the first lecture. This cloud of late-time ionization scatters and polarizes radiation.

The other thing which we might learn about from polarization observations is gravity waves. Thus far we have ignored gravity waves in our discussions.

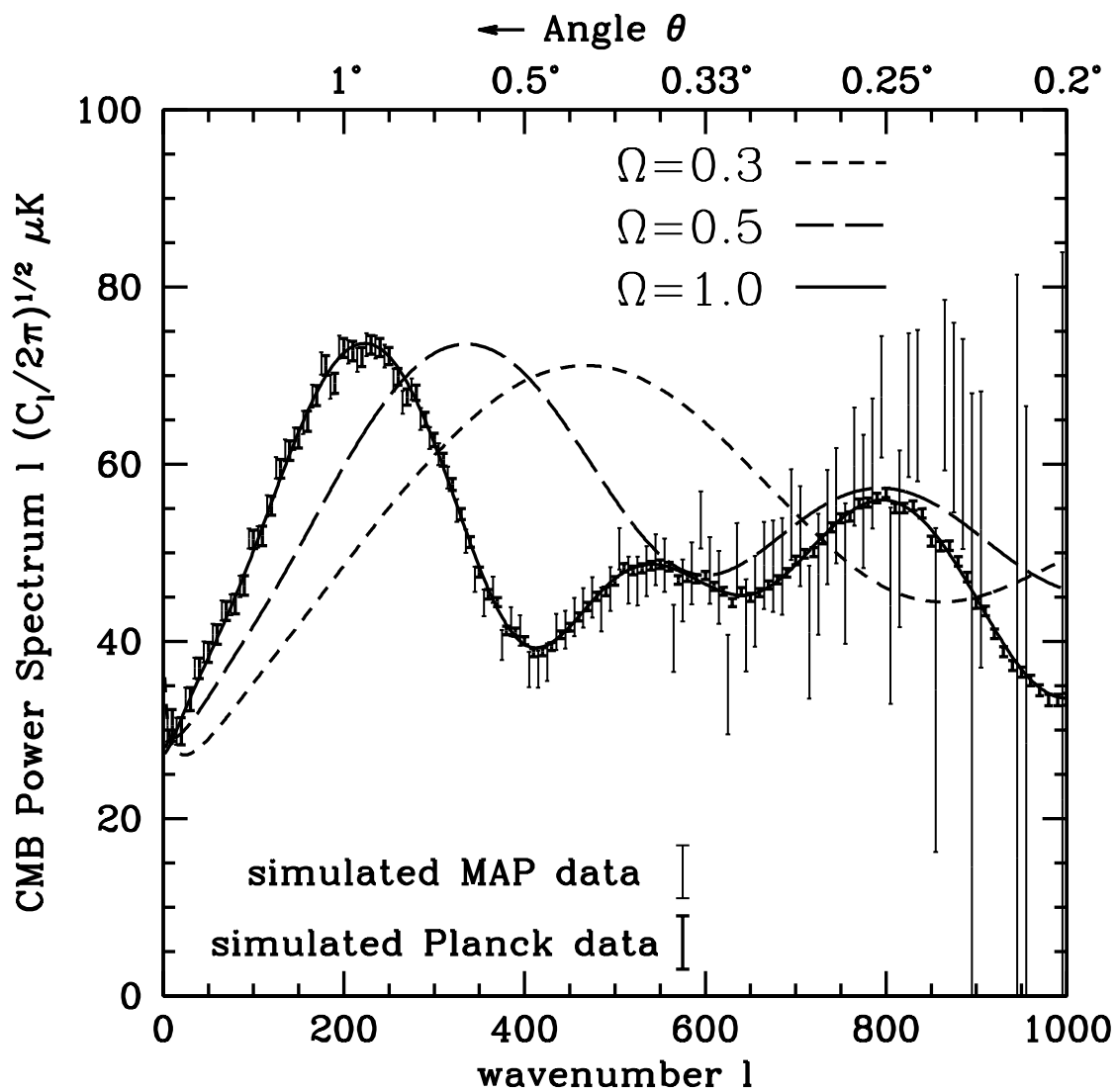


FIGURE 3. Estimated power spectrum sensitivity for MAP and PLANCK. Taken from Ref. [Kam98].

It turns out that it is not too hard to include them in the calculations of the primary temperature anisotropy. They can give a significant contribution to the low l part of the signal because they represent a time-varying gravitational field throughout the time between recombination and the present; think of it as a kind of purely relativistic integrated Sachs-Wolfe effect. The problem is that this low l part of the temperature power spectrum is subject to uncertainty due to cosmic variance. Because of this it may be impossible to extract the signal from this part of the data. However, gravity waves give a contribution to the polarization signal which is detectable at large l as well. So the best way to detect gravity waves may well be to measure the polarization signal.

REFERENCES

- [F⁺96] D. Fixsen et al., *The Cosmic Microwave Background from the Full COBE FIRAS Data Set*, astro-ph/9605054.
- [HSSW95] W. Hu, D. Scott, N. Sugiyama, and M. White, *The Effect of Physical Assumptions on the Calculation of Microwave Background Anisotropies*, astro-ph/9505043.
- [Kam98] M. Kamionkowski, *Cosmological Parameter Determination with Cosmic Microwave Background Temperature Anisotropies and Polarization*, astro-ph/9803168.
- [M⁺02] S. Masi et al., *The BOOMERanG Experiment and the Curvature of the Universe*, astro-ph/0201137.
- [Smo97] G. Smoot, *The CMB Anisotropy Experiments*, astro-ph/9705135.
- [SS97] G. Smoot and D. Scott, *Cosmic Background Radiation*, astro-ph/9711069.
- [Ste97] A. Stebbins, *The CMBR Spectrum*, astro-ph/9705178.